Journal of
Biomedical Nanotechnology
Vol. 1, 90–95, 2005

Vibrational Modes of Nano-Template Viruses

Alexander A. Balandin* and Vladimir A. Fonoberov

Nano-Device Laboratory, Department of Electrical Engineering,
University of California – Riverside, Riverside, California 92521, USA

Viruses have recently attracted attention as biological templates for assembly of nanostructures and nanoelectronic circuits. They can be coated with metals, silica or semiconductor materials and form end-to-end nanorod assemblies. Such viruses as tobacco mosaic virus (TMV) and M13 bacteriophage have appropriate cylindrical shape and particularly suitable dimensions: M13 is 860 nm long and 6.5 nm in diameter, while TMV is 300 nm long, 18 nm in diameter and with a 4 nm in diameter axial channel. The knowledge of vibrational, i.e. quasi-acoustic phonon, modes of these viruses is important for material and structural characterization of the virus-based nano-templates and for *in-situ* control of the nanostructure self-assembly. In this paper we report on calculation of the dispersion relations for the lowest vibrational frequencies of TMV and M13 bacteriophage immersed in air and water. We analyze the damping of vibrations in water and discuss application of micro-Raman spectroscopy for control of the virus-based self-assembly processes.

Keywords: Tobacco Mosaic Virus, Nano-Template Viruses, Micro-Raman Spectroscopy, Nano-Phononics.

RESEARCH ARTICLE

1. INTRODUCTION

Fundamental limitations for the conventional complementary metal-oxide semiconductor (CMOS) technology scaling beyond certain limits motivate the search for alternative fabrication technologies and self-assembly concepts.[1] One of the important problems associated with actively pursued semiconductor self-assembly technique such as stress-driven molecular-beam epitaxy (MBE) self-assembly[2–3] is the size dispersion of the components. It is extremely difficult to manufacture identical or nearly identical structures at nanoscale. The MBE grown nanowires, nanorods or quantum dots, proposed as elements in future nanoelectronic circuits, come with size variation despite serious efforts on size, shape and position control in the last decade or so.[4–5] Self-assembly using chemically produced templates is another promising approach.[6–7] But, though in lesser degree, it also suffers from the same problem: nanopores are also not identical in size.

A most recently proposed nano-fabrication technique,[8–10] which presents a radical departure from conventional approaches, is utilization of biological objects, such as viruses, as nano-templates for the fabrication. Specifically, rod-shaped viruses, such as tobacco mosaic virus (TMV) and M13 bacteriophage, have been utilized as biological templates in the synthesis of semiconductor and metallic nanowires.[8, 10] Genetically modified TMV and M13 viruses have been successfully used for self-assembly of nanomaterials into liquid crystals, films, and fibers.[9] It is expected that genetically programmed viruses will contribute to the next generation of nanoelectronic circuits and optoelectronic devices. Both TMV and M13 viruses have cylindrical shape, which is very convenient for applications as nano-templates (see Fig. 1). M13 bacteriophage is 860 nm long and 6.5 nm in diameter, while TMV is 300 nm long, 18 nm in diameter and with a 4 nm in diameter axial channel.[8]

Since these viruses have the diameters of the same order of magnitude as diameters of semiconductor nanocrystals and nanowires, elastic vibrations of TMV and M13 viruses should manifest themselves in low-frequency Raman scattering spectra. The theoretical understanding of the low-frequency vibrational modes of the viruses is important for interpretation of Raman (Brillouin) spectra and monitoring the aforementioned self-assembly processes. For example, low-frequency vibrational modes of pure

*Author to whom correspondence should be addressed.

 1550-7033/2005/1/090/006/$17.00+.25 doi:10.1166/jbn.2005.005

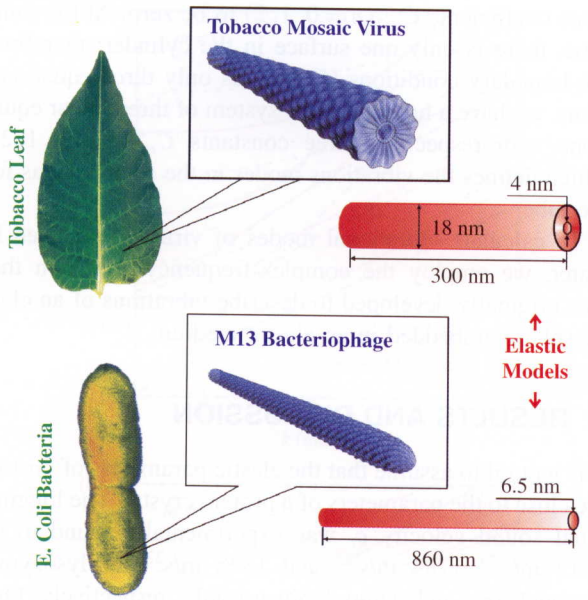

Fig. 1. Illustration of an actual view and simplified models of the tobacco mosaic virus (TMV) and M13 bacteriophage. Virus sizes are shown on the elastic cylinders used for modeling the viruses.

TMV and silica coated TMV are different. The same can be said about low-frequency vibrational modes of a single functionalized TMV nanorod and end-to-end connected assembly of TMV nanorods, which form a nanotubular superstructure.[8] Thus, signatures of these unique vibrational modes observed in Raman (Brillouin) spectra can be used to monitor and help to control the process of virus functionalization, i.e. coating with different materials, and self-assembly, i.e. attachment to other objects such as quantum dots, carbon nanotubes, etc.; or forming end-to-end superstructures. Information, which can be obtained with the help of Raman spectroscopy, is particularly valuable since other direct characterization techniques, such as transmission electron microscopy (TEM), are difficult to carry out and require special treatment of the samples.

Recent developments in molecular biology and instrumentation for Raman spectroscopy have strongly increased the usefulness of the micro-Raman spectroscopy for gaining insights into internal virus structure and viral assembly pathways.[11] At the same time, the Raman spectroscopy of viruses was mostly limited to large wave number region of 600 cm^{-1} and above.[11] The latter is understandable since the main motivation was the study of internal virus composition, localized vibrations of multiply bonded or electron-rich groups in proteins, or viral assembly pathways. Here, our task is different. We look at viruses as generic cylindrical nano-rods used as templates, and will utilize the obtained information on their quasi-acoustic vibrations for interpretation of experimental Raman spectra and extraction of mechanical and structural information of virus-based functionalized assemblies.

There are only few reports on the estimation of vibrational modes in organic nanostructures: spherical virus particles have been considered in Refs. [12, 13] and thin-wall microtubules have been studied in Ref. [14]. Preliminary results for the rod-shaped viruses were reported by us without details of the calculations.[15] Here, we present results of our calculations of phonon spectra of TMV and M13 viruses immersed in air and water. Results for water are important since this is the medium of virus synthesis, purification and assembly processes. Water is also a notoriously strong infrared (IR) absorbing medium, and generally samples can be investigated more favourably by Raman rather than by Fourier transform infrared (FTIR) methods. The rest of the paper is organized as follows. In Section 2 we present our analytical approach to modeling of vibrational modes in cylindrically-shaped viruses. Results and discussion are presented in Section 3. We give our conclusions in Section 4.

2. ANALYTICAL APPROACH

Taking into account the size and shape of the viruses (M13 bacteriophage is 860 nm long and 6.5 nm in diameter, while TMV is 300 nm long, 18 nm in diameter) we employ elastic continuum approximation. It has been shown that continuum approach works remarkably well even for nanometer thick semiconductor structures and single wall carbon nanotubes.[16–17] Due to the fact that the length of the viruses is much larger than their diameter, we model TMV and M13 as infinite cylinders (see Fig. 1).

The low-frequency vibrational modes of cylindrical viruses are found as eigenmodes of the equation of motion for the displacement vector **u**. Due to the axial symmetry of the problem, the equation of motion can be solved analytically in cylindrical coordinates (r, ϕ, z). First, we present the solution of the equation of motion for a free-standing elastic cylindrical tube with the internal radius R_1 and the external radius R_2 (for TMV $R_1 = 2$ nm and $R_2 = 9$ nm). Then, we explain how to take the limit $R_1 \to 0$ (the case of M13) and how to consider the case of an elastic tube immersed in water.

The displacement vector that satisfies the equation of motion for an elastic cylindrical tube can be written as:[18]

$$\begin{aligned} u_r &= \left(\frac{dG(r)}{dr} - \frac{m}{r}F_1(r) + k\frac{dF_2(r)}{dr}\right) \\ &\quad \times \cos(m\phi)\cos(kz)e^{i\omega t} \\ u_\phi &= \left(-\frac{m}{r}G(r) + \frac{dF_1(r)}{dr} - k\frac{m}{r}F_2(r)\right) \\ &\quad \times \sin(m\phi)\cos(kz)e^{i\omega t} \\ u_z &= (-kG(r) + k_t^2 F_2(r))\cos(m\phi)\sin(kz)e^{i\omega t} \end{aligned} \tag{1}$$

RESEARCH ARTICLE

where

$$G(r) = C_{0,1}J_m(k_l r) + C_{0,2}N_m(k_l r)$$
$$F_n(r) = C_{n,1}J_m(k_t r) + C_{n,2}N_m(k_t r) \qquad (n = 1, 2) \tag{2}$$

$$k_l^2 = \frac{\omega^2}{c_l^2} - k^2; \qquad k_t^2 = \frac{\omega^2}{c_t^2} - k^2 \tag{3}$$

In Eqs. (1)–(3), m is the angular quantum number, k is the axial wavenumber, ω is the vibrational frequency; J_m and N_m are Bessel functions of the first and second kind; and c_l and c_t are longitudinal and transverse velocities of sound, respectively. Note that in addition to Eq. (1) there are three more forms of the solution of the equation of motion. These forms can be obtained by applying to Eq. (1) one or two of the transformations:

$$\begin{cases} \cos(m\phi) \to \sin(m\phi), \\ \sin(m\phi) \to -\cos(m\phi); \end{cases} \qquad \begin{cases} \cos(kz) \to \sin(kz) \\ \sin(kz) \to -\cos(kz) \end{cases} \tag{4}$$

There are six independent constants $C_{i,j}$ in Eq. (1) [see Eq. (2)]. To find these constants for the case of a free-standing tube (immersed in air) we have to apply the boundary conditions that the radial components of the stress tensor τ vanish on both internal and external surfaces of the tube:

$$\tau_{r\alpha}|_{r=R_j} = 0 \qquad (\alpha = r, \phi, z; \quad j = 1, 2) \tag{5}$$

where

$$\tau_{rr} = \rho\left[c_l^2 \frac{\partial u_r}{\partial r} + (c_l^2 - 2c_t^2)\left(\frac{u_r}{r} + \frac{1}{r}\frac{\partial u_\phi}{\partial \phi} + \frac{\partial u_z}{\partial z}\right)\right]$$
$$\tau_{r\phi} = \rho c_t^2\left(\frac{1}{r}\frac{\partial u_r}{\partial \phi} + \frac{\partial u_\phi}{\partial r} - \frac{u_\phi}{r}\right) \tag{6}$$
$$\tau_{rz} = \rho c_t^2\left(\frac{\partial u_r}{\partial z} + \frac{\partial u_z}{\partial r}\right)$$

and ρ is the mass density. Thus, one has a homogeneous system (5) of six linear equations with respect to six constants $C_{i,j}$. The obtained system has nonzero solutions only when the determinant of this system is equal to zero. The above determinant is a function of the vibrational frequency ω; therefore, the zeros of this determinant define a discrete spectrum of vibrational frequencies and the resulting sets of constants $C_{i,j}$ define corresponding displacement vectors (1). Note that the displacement vector (1) is defined to an arbitrary multiplier, which is found by normalizing the displacement vector to unity.

For the free-standing viruses without an internal channel, e.g. M13 bacteriophage in air, the solution of the equation of motion can be obtained in the similar way. Since in this case we have a cylinder instead of the tube, the displacement vector (1) should be finite at $r = 0$. Taking into account the fact that the Bessel function N_m in Eq. (2) diverges at $r = 0$, the above condition requires three coefficients $C_{n,2}(n = 0, 1, 2)$ to be zero. At the same time, there is only one surface in the cylinder; therefore, the boundary conditions (5) give us only three equations. Thus, we have a homogeneous system of three linear equations with respect to three constants $C_{n,1}(n = 0, 1, 2)$, which defines the vibrations modes in the same way as for the tube.

To calculate vibrational modes of viruses immersed in water, we employ the complex-frequency approach that was originally developed to describe vibrations of an elastic sphere embedded in an elastic medium.[19–20]

3. RESULTS AND DISCUSSION

It is natural to assume that the elastic parameters of viruses are close to the parameters of a protein crystal. The longitudinal sound velocity c_l was experimentally found to be 1817 m/s,[21] 1784 m/s,[22] and 1828 m/s[22] for lysozyme, ribonuclease, and hemoglobin crystals, respectively. One can see that the elastic parameters of different protein crystals have close values. For definiteness, we assume that the elastic parameters of viruses coincide with the parameters of lysozyme protein crystal from Ref. [21]. The values of all elastic parameters used in our simulations are summarized in Table I.

The Raman intensity of vibrational modes in cylindrical viruses depends on the polarization of incoming and outgoing light. When both the incoming and outgoing light are polarized along the viral axis, only vibrations with circumferential quantum number $m = 0$ and axial quantum number $k = 0$ can be observed in the Raman spectrum. In the case of the crossed polarization, only vibrations with $m = \pm 1$ and $k = 0$ can be Raman active. Finally, when both the incoming and outgoing light are polarized perpendicularly to the viral axis, only vibrations with $m = 0$; ± 2 and $k = 0$ can give nonzero Raman intensities. On the other hand, the dispersion of vibrational frequencies (dependence on k) is important for calculation of the vibrational density of states. Based on the above facts, we study in detail the vibrational modes with $m = 0, \pm 1, \pm 2$ and their k-dependence.

Figures 2 and 3 show the calculated lowest-frequency dispersion curves for vibrations with $m = 0, \pm 1, \pm 2$ for M13 and TMV, respectively. As one can see from Eqs. (1) and (4), vibrational modes with $m = 0$ can be divided into radial-axial ($u_\phi = 0$) and torsional modes ($u_r = 0$ and $u_z = 0$). While the torsional vibrations have the same frequencies for the viruses immersed in air and water, the

Table I. Sound velocities and mass densities for viruses and water used in the simulation.

	c_l (m/s)	c_t (m/s)	ρ (g/cm^3)
virus	1817	915	1.21
water	1483	0	1

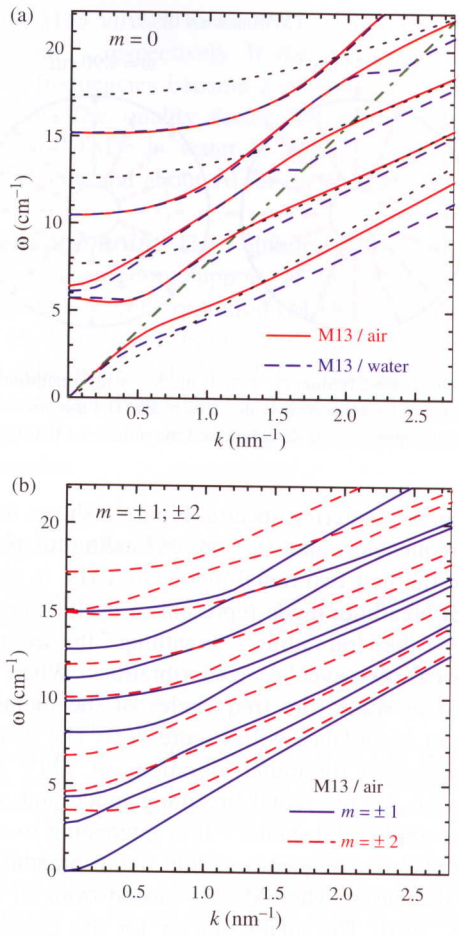

Fig. 2. Dispersion of the lowest vibrational frequencies with circumferential quantum numbers $m = 0, \pm 1, \pm 2$ for M13 bacteriophage. (a) Solid (dashed) lines correspond to the radial-axial vibrations with $m = 0$ in air (water). Dotted lines correspond to the torsional vibrations with $m = 0$. Dash-dotted line marks the sound velocity of water. (b) Solid (dashed) lines correspond to the elastic vibrations with $m = \pm 1 (m = \pm 2)$ in air.

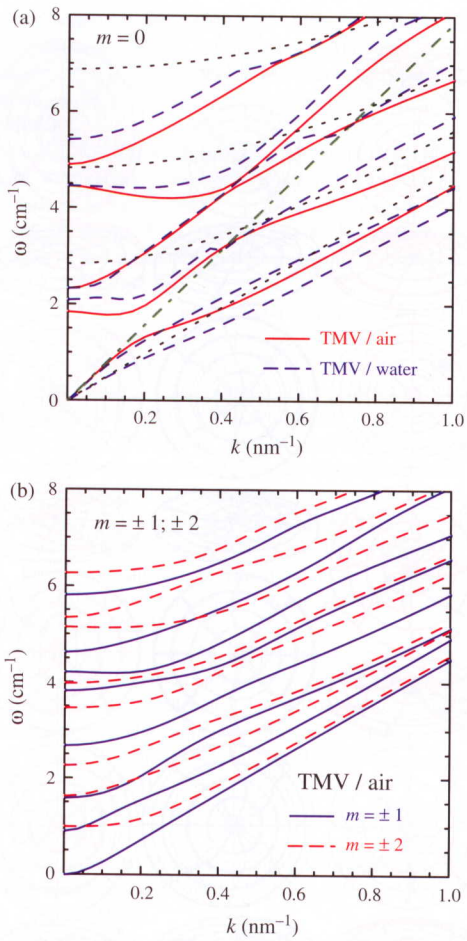

Fig. 3. Dispersion of the lowest vibrational frequencies with circumferential quantum numbers $m = 0, \pm 1, \pm 2$ for tobacco mosaic virus. Notations are the same as in Figure 2.

radial-axial vibrations are different. The main difference consists in the fact that radial-axial vibrations in air are harmonic while radial-axial vibrations in water are damped when $\omega > kc_l^{(\text{water})}$, i.e. the frequency has a nonzero imaginary part that is equal to the inverse lifetime and also defines the broadening of the Raman peak. When both $m = 0$ and $k = 0$, the radial-axial vibrations split into purely radial and purely axial, as seen from Eqs. (1) and (4). The radial vibrational mode with the lowest frequency is called the radial breathing mode. Like torsional modes, axial modes with $k = 0$ are not damped and are the same when the exterior medium is air or water. On the contrary, the damping is in its maximum for radial modes with $k = 0$. Comparing Figures 2 and 3, one can see that the presence of the axial channel in TMV substantially changes the low-frequency vibrational modes. For example, the lowest radial-axial acoustical branch of M13 in water splits in two parts for TMV in water. Moreover, there is only one radial mode in Figure 2(a), while there are two such modes in Figure 3(a). Finally, the radial mode is the mode with the lowest nonzero frequency for TMV, while it is the second lowest nonzero frequency for M13.

Since the vibrational modes with $m = 0, \pm 1, \pm 2$ and $k = 0$ can be observed in the Raman scattering spectra, it is important to visualize the displacements **u** corresponding to such vibrations. It is seen from Eqs. (1) and (4) that the displacement **u** does not depend on the variable z when $k = 0$. Therefore, it is enough to visualize the vibrations of a circular viral cross-section. Figure 4 presents such visualization for vibrations of M13 in air. Other cases, such as vibrations of TMV or vibrations in water can be considered analogously. For the eigenfunctions shown in Figure 4, the corresponding vibrational frequencies increase from top to bottom; the values of these frequencies can be found in Figure 2 ($k = 0$). The first two vibrational modes with $m = 0$ and the first vibrational mode with $m = 1$ have zero frequencies and correspond to the rigid body motions. The 3rd, 6th, and 8th modes with $m = 0$ as well as the 2nd, 4th, and 7th modes with $m = 1$ and 2 are axial vibrations. The fourth mode with $m = 0$ is the radial breathing mode, while the 5th, 7th, and 9th modes with $m = 0$ are torsional

RESEARCH ARTICLE

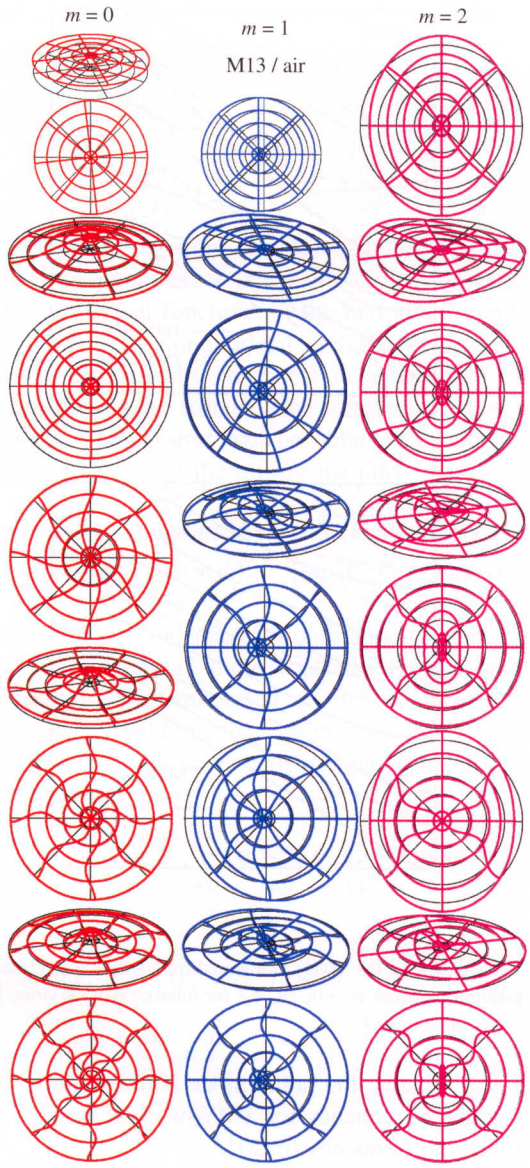

Fig. 4. Schematic pictures of the viral cross-section displacements for vibrations with quantum numbers $k = 0$ and $m = 0, 1, 2$ of M13 bacteriophage in air. Displacements for vibrations with $m = -1 (m = -2)$ can be obtained by rotating the displacements shown for $m = 1 (m = 2)$ by 90° (45°) around the symmetry axis normal to the viral cross-section. The equilibrium position is shown with thin lines. The thick lines show the maximum deviation from the equilibrium. The corresponding vibrational frequencies increase from top to bottom. The values of the frequencies are shown in Figure 2 ($k = 0$). Note that three small cross-sections have zero vibrational frequency and correspond to the rigid body motions.

vibrations. The first and sixth modes with $m = 2$ represent vibrations that squeeze the entire virus in one direction, while the 3rd, 5th, and 8th modes with $m = 2$ correspond to vibrations, where only the central part of the virus is periodically squeezed. The remaining four modes with $m = 1$ have a distinct translational vibration of the central part of the virus.

Radial modes with $m = 0$ and $k \doteq 0$ are particularly important since they usually have the maximum intensity

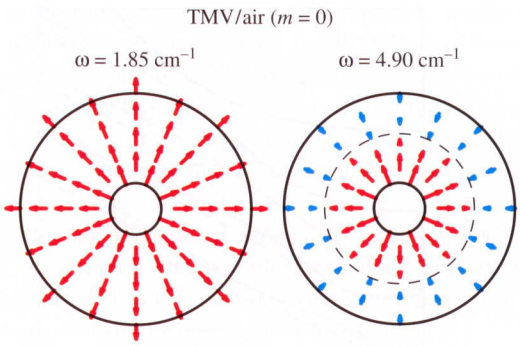

Fig. 5. Two lowest-frequency radial modes with quantum numbers $k = 0$ and $m = 0$ for tobacco mosaic virus in air. The direction and length of arrows correspond to the direction and magnitude of the displacement vector.

in the Raman scattering spectra. Figure 5 shows the vibrational frequencies and the corresponding displacement fields for the first two radial modes of TMV in air. While the radial breathing mode represents a cyclic increase and decrease of the viral radius – "breathing," the second radial mode reveals two synchronized vibrations. When TMV is immersed in water, the frequencies of the radial modes increase in accordance with Figure 3(a). The quality factor $\mathrm{Re}(\omega)/\mathrm{Im}(\omega)$ for radial vibrations of TMV in water is about 3.6 for the radial breathing mode and about 10 for the second radial mode.[15] It is interesting to note that unlike TMV, the frequency of the radial breathing mode of M13 decreases, when M13 is moved from air to water [see Fig. 2(a)]. The quality factor for the radial breathing mode of M13 is also about 3.6.[15] The relatively large quality factor for radial vibrations of M13 and TMV in water allows one to observe these vibrations in the Raman spectrum, despite the damping.

Calculated low-frequency vibrational modes of TMV and M13 viruses are required for interpretation of the low-frequency Raman (Brillouin) scattering spectra from pure viruses and viruses coated with some materials. The differences in Raman spectra can be used to monitor the coating and nano-assembly process. It may also help to assess how successful the virus coupling to quantum dots or other elements of nano-assemblies in a process similar to the one reported for carbon nanotubes-quantum dots assemblies.[23] Further investigation of the low-frequency vibrational modes in nano-template viruses may lead to the development of *in-situ* process monitoring of the self-assembly process of the hybrid nanoelectronic circuits.

4. CONCLUSIONS

In conclusion, we investigated vibrational modes of TMV and M13 viruses, which have been proposed for utilization as nano-templates for chemical assembly of nano-electronic components. Obtained information is important for interpretation of Raman (Brillouin) spectra and control of the assembly process. The radial breathing modes of

RESEARCH ARTICLE

TMV and M13 viruses in air are found to be 1.85 cm^{-1} and 6.42 cm^{-1}, respectively. If the viruses are in water, the above frequencies become 2.10 cm^{-1} and 6.12 cm^{-1}, respectively. The quality factor $Re(\omega)/Im(\omega)$ for radial vibrations of TMV in water is about 3.6 for the radial breathing mode and about 10 for the second radial mode.

Acknowledgments: The authors acknowledge the financial and program support of the Microelectronics Advanced Research Corporation (MARCO) and its Focus Center on Functional Engineered Nano Architectonics (FENA). The authors also thank K. Alim and A. Morgan, members of the Nano-Device Laboratory (http://ndl.ee.ucr.edu/), for useful comments on Raman spectroscopy of TMV samples.

References and Notes

1. The Semiconductor Industry Association: International Technology Roadmap for Semiconductors (**2003**). SRC website at http://www.src.org/.
2. J. L. Liu, W. G. Wu, A. Balandin, G. Jin, and K. L. Wang, Intersubband absorption in boron-doped multiple Ge quantum dots, *Appl. Phys. Lett.* 74, 185 (**1999**).
3. J. L. Liu, W. G. Wu, A. Balandin, G. Jin, Y. H. Luo, S. G. Thomas, Y. Lu, and K. L. Wang, Observation of inter-sub-level transitions in modulation-doped Ge quantum dots, *Appl. Phys. Lett.* 75, 1745 (**1999**).
4. T. I. Kamins and R. S. Williams, Lithographic positioning of self-assembled Ge islands on Si(001), *Appl. Phys. Lett.* 71, 1201 (**1997**).
5. A. Balandin, G. Jin, and K. L. Wang, Issues of practical realization of a quantum dot register for quantum computing, *J. Electronic Materials* 29, 549 (**2000**).
6. S. Bandyopadhyay, A. E. Miller, H. C. Chang, G. Banerjee, D. F. Yue, R. E. Ricker, S. Jones, J. A. Eastman, and M. Chandrasekhar, Electrochemically assembled quasi-periodic quantum dot arrays, *Nanotechnology* 7, 360 (**1996**).
7. A. Balandin, K. L. Wang, N. Kouklin, and S. Bandyopadhyay, Raman spectroscopy of electrochemically self-assembled CdS quantum dots, *Appl. Phys. Lett.* 76, 137 (**2000**).
8. W. Shenton, T. Douglas, M. Young, G. Stubbs, and S. Mann, Inorganic-organic nanotube composites from template mineralization of tobacco mosaic virus, *Adv. Mater.* 11, 253 (**1999**).
9. C. E. Flynn, S. W. Lee, B. R. Peelle, and A. M. Belcher, Viruses as vehicles for growth, organization and assembly of materials, *Acta Materialia* 51, 5867 (**2003**); C. Mao, D. J. Solis, B. D. Reiss, S. T. Kottmann, R. Y. Sweeney, A. Hayhurst, G. Georgiou, B. Iverson, and A. M. Belcher, Virus-based toolkit for the directed synthesis of magnetic and semiconducting nanowires, *Science* 303, 213 (**2004**).
10. M. Knez, A. M. Bittner, F. Boes, C. Wege, H. Jeske, E. Maiss, and K. Kern, Biotemplate synthesis of 3-nm nickel and cobalt nanowires, *Nano Letters* 3, 1079 (**2003**); M. Knez, M. Sumser, A. M. Bittner, C. Wege, H. Jeske, T. P. Martin, and K. Kern, Spatially selective nucleation of metal clusters on the tobacco mosaic virus, *Adv. Funct. Mater.* 14, 116 (**2004**).
11. R. Tuma and G. J. Thomas, *Raman Spectroscopy of Viruses, in Handbook of Vibrational Spectroscopy*, edited by J. M. Chalmers and P. R. Griffiths, John Wiley & Sons, Chichester (**2002**).
12. L. H. Ford, Estimate of the vibrational frequencies of spherical virus particles, *Phys. Rev. E* 67, 051924 (**2003**).
13. L. Saviot, D. B. Murray, A. Mermet, and E. Duval, Comment on estimate of the vibrational frequencies of spherical virus particles, *Phys. Rev. E* 69, 023901 (**2004**).
14. Y. M. Sirenko, M. A. Stroscio, and K. W. Kim, Elastic vibrations of microtubules in a fluid, *Phys. Rev. E* 53, 1003 (**1996**).
15. V. A. Fonoberov and A. A. Balandin, Low-frequency vibrational modes of viruses used for nanoelectronic self-assemblies, *Phys. Stat. Sol. B* 241, R67 (**2004**).
16. A. Raichura, M. Dutta, and M. A. Stroscio, Quantized acoustic vibrations of single-wall carbon nanotube, *J. Appl. Phys.* 94, 4060 (**2003**).
17. E. Dobardzic, J. Maultzsch, I. Milosevic, C. Thomsen, and M. Damnjanovic, The radial breathing mode frequency in double-walled carbon nanotubes: An analytical approximation, *Phys. Stat. Sol. B* 237, R7 (**2003**).
18. K. F. Graff, *Wave Motion in Elastic Solids*, Dover Publications, New York (**1991**).
19. V. A. Dubrovsky and V. S. Morochnik, Normal-modes of a spherical inclusion within an elastic medium, *Izv. Acad. Sci. USSR, Phys. Solid Earth* 17, 494 (**1981**).
20. D. B. Murray and L. Saviot, Phonons in an inhomogeneous continuum: Vibrations of an embedded nanoparticle, *Phys. Rev. B* 69, 094305 (**2004**).
21. M. Tachibana, K. Kojima, R. Ikuyama, Y. Kobayashi, and M. Ataka, Sound velocity and dynamic elastic constants of lysozyme single crystals, *Chem. Phys. Lett.* 332, 259 (**2000**).
22. C. Edwards, S. B. Palmer, P. Emsley, J. R. Helliwell, I. D. Glover, G. W. Harris, and D. S. Moss, Thermal motion in protein crystals estimated using laser-generated ultrasound and young's modulus measurements, *Acta Crystallogr., Sect. A: Found. Crystallogr.* A46, 315 (**1990**).
23. S. Ravindran, S. Chaudhary, B. Colburn, M. Ozkan, and C. Ozkan, Covalent coupling of quantum dots to multiwalled carbon nanotubes for electronic device applications, *Nano Letters* 3, 447 (**2003**).

Received: 24 September 2004. Accepted: 12 October 2004.